

INCREASE OF AUSTENITIC DUCTILE IRON TYPE D5S DURABILITY BY HIGH TEMPERATURE PRE-TREATMENT

W. J. Nowak ^{a*}, B. Wierzba ^a, A. Mazurkow ^a, A. Jaworski ^b, Ł. Krawczyk ^b

^{a*}Department of Materials Science, Faculty of Mechanical Engineering and Aeronautics, Rzeszow University of Technology, Rzeszow, Poland

^bBorgWarner Turbo Systems, BorgWarner Poland, Rzeszow Technical Center, Poland

(Received 16 December 2019; accepted 06 October 2020)

Abstract

In the present work, a performance of ASTM A439 Austenitic Ductile Iron type D5S at high temperature in the oxidizing environment was investigated. The obtained results revealed that exposure at temperatures 800°C, 850°C, and 900°C resulted in relatively high mass gain and an extensive oxide scale spallation from the samples' surfaces during cooling. However, the material exposed at 950°C revealed a better oxidation resistance and no oxide scale spallation. The material exposed at 1000°C showed the best oxidation resistance among the studied samples. The surfaces and cross-sectional investigation revealed that the material exposed at 950°C formed mostly Ni/Cr/Mn-mixed protective oxide scale and local formation of Fe-rich nodules. In comparison with the sample exposed at 1000°C, a smaller amount of Fe-rich nodules per area unit was observed and most of the surface was covered by Ni/Cr/Mn-mixed protective scale. The latter was explained by the change in the calculated diffusion coefficients in the alloy for Ni and Fe, namely up to 900°C the diffusion coefficient for Fe was much higher than for Ni, while above 900°C the diffusion coefficient for Ni becomes higher than for Fe. This phenomenon was correlated with a phase transformation from α -Fe into γ -Fe resulting in the diffusion coefficient change.

Keywords: Ductile iron; Oxidation kinetics; Automotive turbine housings; Lifetime modification; Temperature effect

1. Introduction

The automotive turbine housings are components used for collecting exhaust gases generated from individual cylinders, directing them to the turbine wheel, and transfer further into the exhaust system. The turbine housing is subjected to the highest loads, partly due to increased mass flow of exhaust gases and partly to additional loads from the weight of the turbocharger. Raw turbine housing oxidation resistance is relevant to the quality of the protective oxide scale, created on its inner surface when corrosive exhaust gases pass through the component. During thermal cycling caused by daily operation of the car engine, stresses arise in the scale, increasing the risk of oxide spallation. Continuous oxidization of material results microscopically in depletion of oxide-forming elements and macroscopically consumption of the metal, leading to degradation of component mechanical properties. It is, therefore, important that the formed oxide scale is protective, adherent, and homogeneous. Then, the formation of an Al_2O_3 or Cr_2O_3 based oxide scale is the most desirable. Surface corrosion also negatively influences the component fatigue life, since simultaneous crack growth and

oxidation is known to be detrimental [1,2,3,4]. Therefore, the turbine housing high durability at high-temperature arises.

Depending on the exhaust gas temperature (usually 700 - 1000°C), the materials available for turbine housings include ferritic and austenitic ductile cast iron alloys and cast stainless steel [5]. Ferritic alloys have the benefit of higher thermal conductivity and a lower coefficient of thermal expansion compared with austenitic alloys. However, the austenitic alloys, on the other hand, are characterized by higher strength at high temperatures, making them a better choice for high-temperature applications due to precipitation hardening [6,7].

The Ni-containing ductile irons belong to a group of austenitic ductile cast irons. The alloy commonly used in turbine housings is the austenitic ductile iron D5S, also referred to EN-GJSA-XNiSiCr35-5-2 or 5.3505, containing the highest Ni content, responsible for austenitic structure in ambient temperature and improvement of high-temperature strength, toughness, and creep properties [8]. Relatively high silicon and chromium contents provide high mechanical properties and erosion resistance by the formation of carbides and self-protective oxide scale

*Corresponding author: w.nowak@prz.edu.pl



[9]. D5S turbine housings operate close to their fatigue and oxidation resistance limits. However, even with superior overall properties, the application of this material is still limited by its rather high cost compared with the other possible alternative materials [9,10].

Ductile iron was already investigated in terms of its mechanical and fatigue properties at temperature range 20 to 1000°C [11,12]. Also, several attempts at descriptions of oxidation resistance of family of ductile iron, including D5S alloy, at high temperature was already performed [13,14,15,16]. However, all the above-mentioned studies for the oxidation resistance were performed at a temperature up to 800°C. Celik et al. [13] found the best oxidation resistance against air oxidation at 650°C was obtained for AISI 409 stainless steel. However, the cast iron SiMo showed better performance at high temperatures in comparison with GGG40. Scheidhauer et al. [14] observed a similar oxidation behavior during air exposure at 820°C for ferritic SiMoAl in comparison with D5S alloy. Ferritic SiMoAl was proposed as a cheaper alternative for D5S alloy. Brady et al. [15] observed a better oxidation resistance for D5S than SiMo alloy during exposure at 650°C in air + 10% H₂O. Moreover, the extensive oxide scale spallation was found during exposure of D5S at 700°C, while for SiMo formed oxide scale remained adherent. Ekström et al. [16] investigated the effect of Cr and Ni addition to SiMo51 alloy. They found that the addition of Cr in the concentration ranging between 0.5 - 1 wt.% improves the oxidation resistance during exposure at temperature 700 – 800°C. On the other hand, a negative effect of Ni addition on the oxidation resistance of alloy was observed.

It is known that the increase the operating temperature results in an increase the efficiency of the turbines [17]. Therefore, the study aims is to investigate the oxidation resistance of material typically used for turbine casing, namely ductile iron D5S for the first time at a temperature range 800-1000°C.

2. Experimental

In the present work high-temperature oxidation behavior of ductile iron D5S, with the composition given in Table 1, was investigated. The chemical

composition measurement performed using arc spark optical emission spectrometer SPECTROMAX revealed that the element contents were in the range of nominal compositions. However, one should notice that the OES measurement revealed the presence of 0.19 wt% of Mg in the alloy. Rectangular shaped specimens with the dimensions of 12 x 20 x 2 mm samples were cut and subsequently ground using SiC sand-papers till 1200 grit. After grinding, all samples were ultrasonically cleaned in acetone. Then the samples were oxidized in thermogravimetric furnace Xerion XTUBE for 48 hours in air at five different temperatures, namely 800, 850, 900, 950, and 1000°C. The samples were investigated after exposure by laser profilometer Sensofar S-Neox Non-contact 3D Optical Profiler with a vertical resolution of 1 nm and scanning electron microscopy (SEM) ZEISS Field-Emission Gemini SEM 300 equipped and correlated with Bruker Quantax EDS detector was used for SEM/EDX analyses. Images were taken with the use of backscattered electrons (BSE) detector under different magnifications and 20kV acceleration voltage. The EDS detector enabled chemical composition analyses in micro-areas (chemical composition analysis, elements concentration mapping, and line analyses). After surface investigation, samples were covered by a thin gold layer, subsequently electroplated with nickel, and mounted in epoxy resin. Metallographic cross-sections were prepared by a series of grinding and polishing steps with the final step of polishing using the SiO₂ suspension with 0.25 µm granulation. The cross-sections were investigated by light optical microscope (LOM) Nikon ECLIPSE MA200 Inverted Metallurgical Microscope and scanning electron microscope (SEM). The mass change curves were created by Xerion X-tube thermogravimetric furnace. The mass change curves were obtained “in-situ” during oxidation. The mass of the samples was measured and recorded continuously during exposure. After exposure the mass change plots were corrected considering the so-called Archimedes effect. Considering the character of isothermal thermogravimetric oxidation test, only one sample was tested during one campaign (i.e. one sample was exposed during one run at certain temperature). However, to check and ensure repeatability of obtained results, a second run of oxidation test at the

Table 1. Nominal and measured chemical composition of studied ductile iron D5S (wt%) according to ASTM A439-83(2004) standard and compared with EN 13835 specification

Elements	C	Si	Mn	Ni	Cr	P	Cu	S	Mo	Nb	Mg	Fe
EN 13835	max. 2.0	4.0 – 6.0	0.5 – 1.5	34.0 – 36.0	1.5 – 2.5	max. 0.08	max. 0.50	ND*				balance
Measured	1.9	4.8	0.7	34.5	1.9	0.03	0.02	0.01	0.04	0.01	0.19	55.93

ND* - not defined in EN 13835 specification and in ASTM A439-83(2004) standard



same temperature was performed. This means that for each temperature two samples were investigated. The obtained results showed no discrepancies, therefore, only one result per each exposure temperature was shown in the present work. The information about specimens' surface topography (textures and profiles) was obtained using Sensofar S neoX optical 3D profiling microscope by interferometry measurement technique. Nikon 10X DI objective lens were used. Image post processing was carried out using Mountains® surface texture metrology software.

3. Results

3.1. Material in the as-received condition

The microstructure of the studied alloy is shown in Figure 1. The microphotograph revealed the presence of spheroids of the graphite within the austenitic matrix. The graphite nodules did not exhibit perfectly round shapes, but had sharp edges with diameters about 20 μm . Additionally, the interdendritic mixture of chromium carbides and silicide particles was observed (Figure 2a). Moreover, the eutectics were

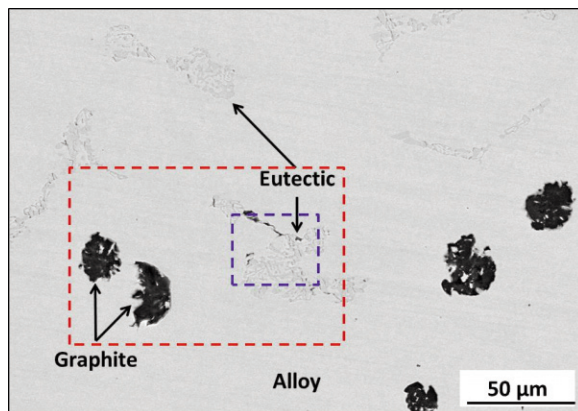
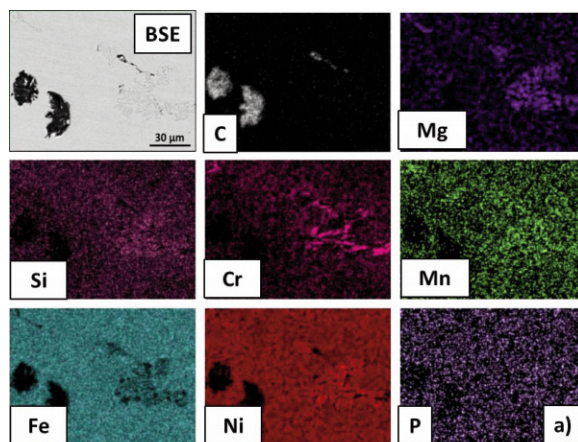


Figure 1. Alloy microstructure in the as-cast conditions performed by light optical microscope



observed in the metallic matrix. In the eutectic co-enrichment of Ni, Cr, Si, Mg, and Mn elements were observed in the form of precipitates in the Fe-rich matrix (Figure 2b).

3.2. Post-exposure analysis

3.2.1. Thermogravimetric analysis

Figure 3 shows the mass changes obtained for the alloy investigated at various temperatures. The mass change obtained at the end of exposure at 800°C (48 h) was equal to 8 $\text{mg}\cdot\text{cm}^{-2}$. The increase of temperature from 800 to 850°C resulted in an increase mass change to 10 $\text{mg}\cdot\text{cm}^{-2}$ and further temperature increase to 900°C resulted in an increase mass change up to 12.5 $\text{mg}\cdot\text{cm}^{-2}$. Despite the relatively high mass change, extensive spallation of the oxide scale during cooling outside the furnace was observed for all samples exposed at the above-mentioned temperature as well. Surprisingly, increasing exposure temperature up to 950°C resulted in a much lower mass change of

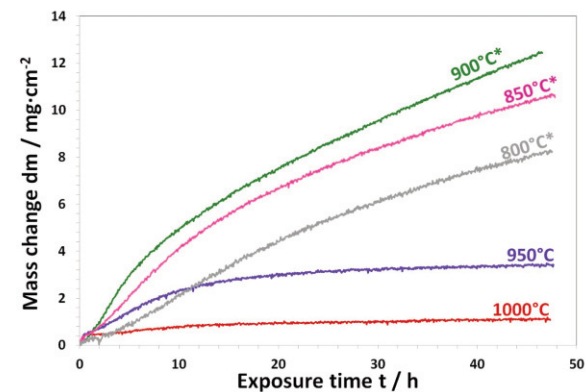


Figure 3. Mass change curves obtained during air oxidation of studied alloy for 48 hours at various temperatures. For the samples exposed at temperature marked with stars an intensive oxide scale spallation during cooling was observed

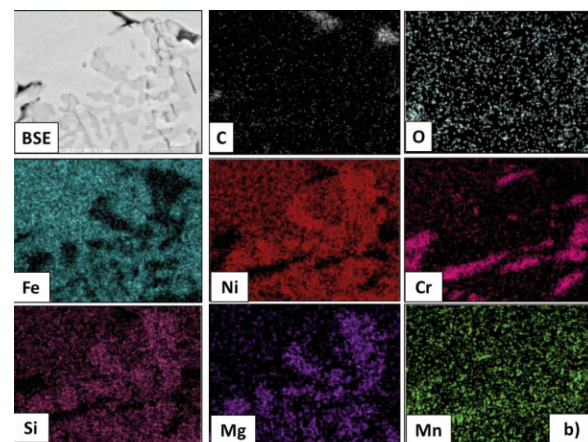


Figure 2. BSE image (upper left image) and elemental maps obtained for studied alloy in the as-cast conditions from: a) region marked by red dashed box and b) region marked by blue dashed box in Fig. 1

studied material as compared to exposure at a lower temperature. For the alloy exposed at 950°C obtained mass change after 48 hours was equal to 3 mg·cm⁻². Further increasing of exposure temperature to 1000°C resulted in a further decrease in obtained mass change at the end of the test, and was equal to 1 mg·cm⁻². Moreover, no oxide scale spallation during cooling of studied material after exposure at 950 and 1000°C was observed, in both cases oxide scale remained adherent. Since the extensive oxide scale spallation at 800°C, 850°C, and 900°C was observed, only specimens exposed at 900°C, 950°C, and 1000°C were further investigated in detail.

3.2.2. Surface investigation

The SEM/SE images of the surfaces of studied material after exposure at 900°C (Figure 4a), 950°C (Figure 4b), and 1000°C (Figure 4c) are shown. The SEM/SE image of the surface of the sample exposed at 900°C revealed the presence of light areas

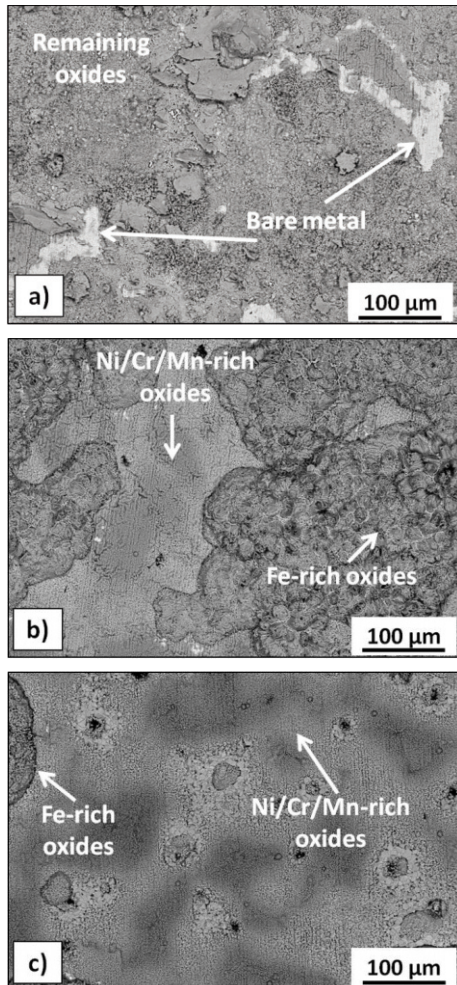


Figure 4. SEM/SE images of the surfaces of the studied alloy after air exposure for 48 hours at: (a) 900°C, (b) 950°C and (c) 1000°C

identified as bare metal. Moreover, there were visible crushed oxides remnants in many places. This was the result of an oxide scale spallation during the cooling stage. The SEM/SE images of the surfaces of samples exposed at 950°C and 1000°C showed that the material tested at both temperatures formed similar oxide scale morphology, namely flat areas and oxide islands were observed. The SEM/EDS analysis showed that the flat surfaces consisted of Ni/Cr/Mn-rich oxide, whereas the oxide islands were identified as Fe-oxides. Such elemental distribution was confirmed by SEM/EDS elemental maps performed for material exposed at 950°C (Figure 5) and 1000°C (Figure 6). However, it is important to point out that the amount of Fe-rich oxide nodules was far less on the surface of material exposed at 1000°C (Figure 4c) compared to the sample exposed at 950°C (Figure 4b). The higher amount of Fe-rich nodules per unit area for sample exposed at 950°C than 1000°C was additionally confirmed by the three-dimensional reproduction by the laser profilometer shown in Figure 7.

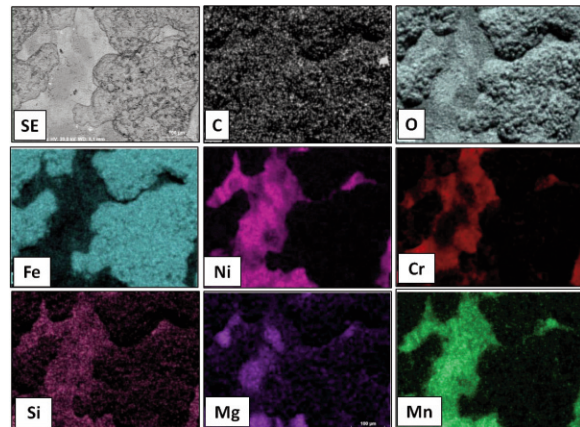


Figure 5. SE image (upper left image) and elemental maps obtained on surface of studied alloy after air oxidation at 950°C for 48 hours

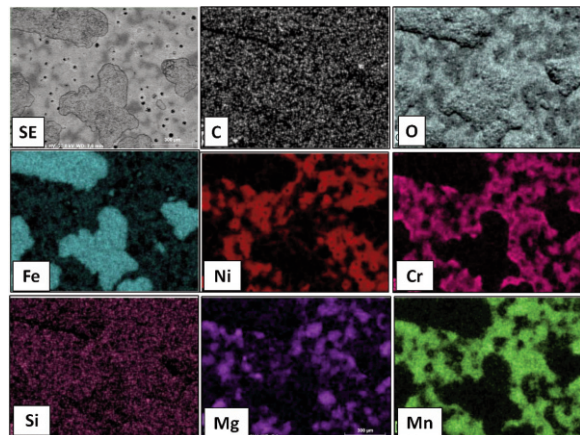


Figure 6. SE image (upper left image) and elemental maps obtained on surface of studied alloy after air oxidation at 1000°C for 48 hours

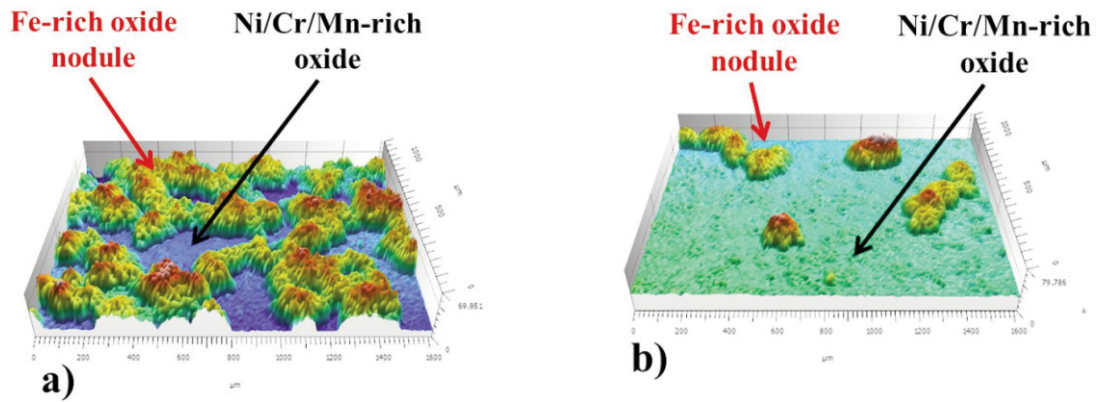


Figure 7. Reproduction of the surface of D5S after air oxidation for 48 hours at: (a) 950 and (b) 1000°C performed by laser profilometer

3.2.3. Cross-sectional investigation

Figure 8 shows SEM/SE images of the studied alloy surfaces after air exposure for 48 hours at 900°C

(a, b), 950°C (c, d), and 1000°C (e, f) taken at low (a, c, e) and high ((b, d, f) magnification. As shown in Figures 8a and 8b, only the internal oxidation zone is visible. However, there are regions where a thin oxide scale formed and regions where relatively thick

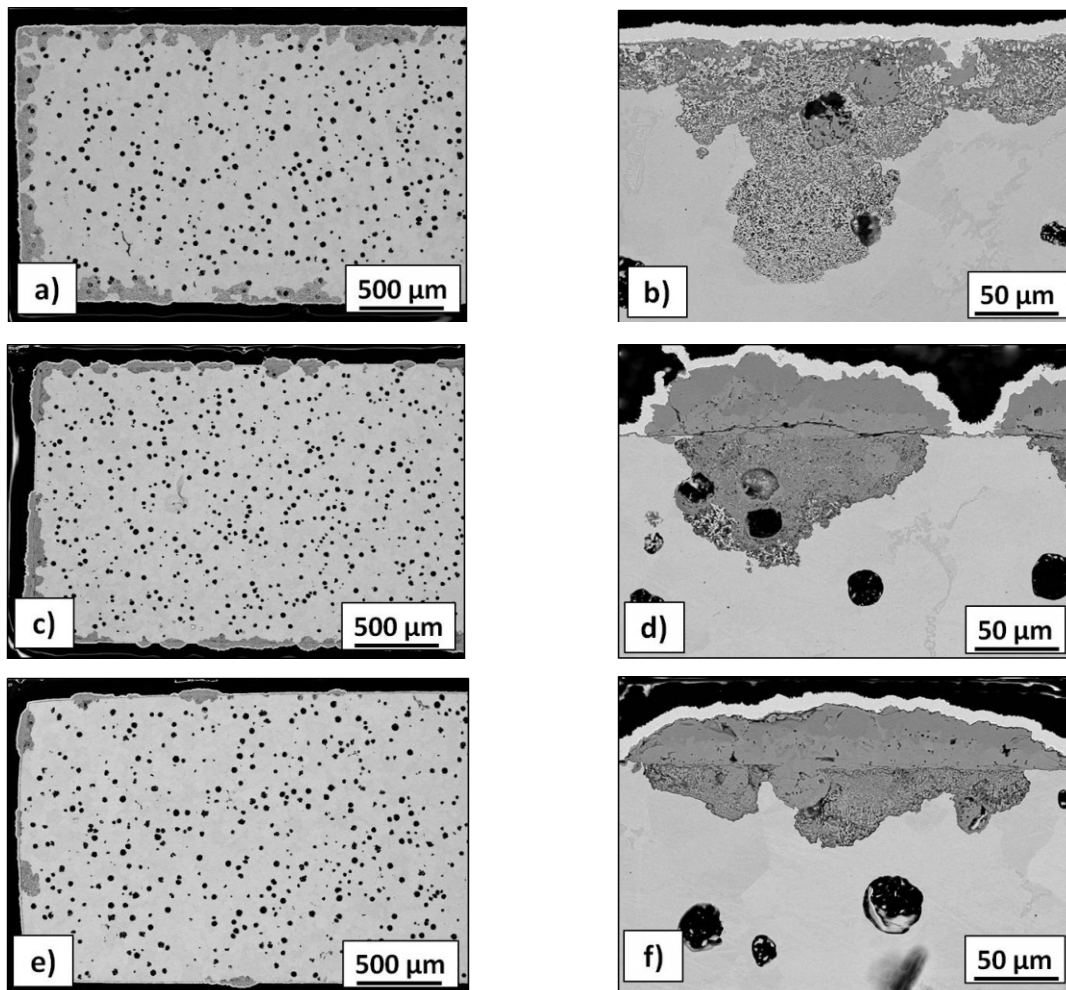


Figure 8. SEM/SE images of the surfaces of studied alloy after air exposure for 48 hours at: (a, b) 900°C, (c, d) 950°C and (e, f) 1000°C taken at low (a, c, e) and high ((b, d, f) magnification

nodules were present on the cross-sections of samples exposed at 950°C and 1000°C (Figure 4 c-f). However, similarly to the observed changes on surfaces, also a smaller number of Fe-rich oxide nodules were present in the cross-sections in the material exposed at 1000°C (Figure 8e) in comparison with material exposed at 950°C (Figure 8c). The SEM/EDS elemental map (Figure 9) revealed that the region of internal oxidation of material exposed at 900°C was enriched in Ni and Si. It could be assumed that Si and Ni were internally oxidized. The SEM elemental maps obtained for samples exposed at 950°C (Figure 10) and 1000°C (Figure 11) showed the formation of the oxide scale with a similar microstructure. Namely, in both cases, regions with a thin continuous oxide scale rich in Ni, Cr, and Mn, and regions with Fe-rich nodules were observed. However, contrary to observations on the sample exposed at 900°C, the formation of continuous sub-scale enriched in Ni, Cr, and Mn at the bottom of the

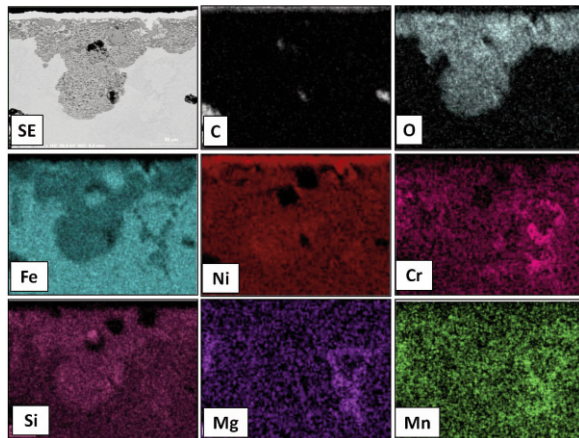


Figure 9. SE image (upper left image) and elemental maps obtained on cross-sections of studied alloy after air oxidation at 900°C for 48 hours

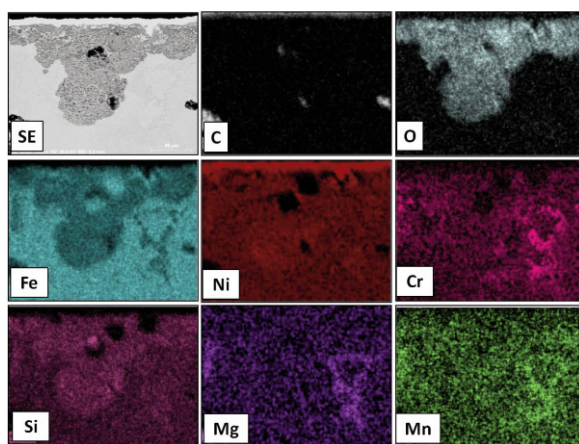


Figure 10. SE image (upper left image) and elemental maps obtained on cross-sections of studied alloy after air oxidation at 950°C for 48 hours

nodule were found. Additionally, in the region of internal oxidation, an enrichment in Ni and Si were present as well. The formation of Ni/Cr/Mn-rich sub-layer was responsible for better oxidation resistance at 950°C and 1000°C, which was indicated by lower mass changes, better oxide scale adhesion, and a smaller number of Fe-rich nodules.

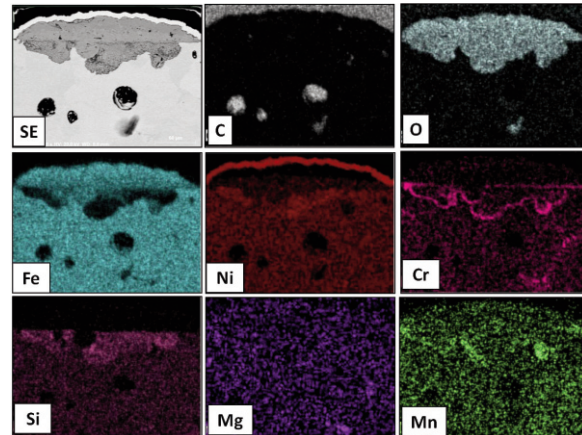


Figure 11. SE image (upper left image) and elemental maps obtained on cross-sections of studied alloy after air oxidation at 1000°C for 48 hours

4. Discussion

As shown above, an increase of exposure temperature from 800°C to 850°C and further to 900°C increased oxidation kinetics (expressed by the mass change). The relatively high mass change resulted in oxide scale spallation during samples cooling. Considering relatively high mass changes obtained for the mentioned temperatures, it can be assumed that the thickness of the formed external oxide scale was higher than the critical oxide scale thickness [10]. The latter resulted in stress accumulation and at the level for which stress relaxation was done by the cracks nucleation and propagation due to crossing so called “critical oxide scale thickness” [18]. Since the difference in coefficients of thermal expansion (CTE) for the oxide scale (ceramic material) and the metallic substrate was relatively high, the stresses near the oxide scale/substrate interface occurred during cooling [19]. At some point, the stress level was so high that the system could relax only by the cracks initiation and propagation. The latter resulted in an extensive oxide scale spallation. However, during exposure conducted at 950°C and 1000°C, no oxide scale spallation was observed. Moreover, the amount of Fe-rich nodules decreased with increasing temperature from 950°C to 1000°C. The better oxidation resistance was correlated with the formation of Ni/Cr/Mn-mixed oxide scale on larger areas (Figures 5, 6, and 7) accompanied with the formation of Cr/Mn-mixed

subscale beneath the Fe-rich oxide scale (Figures 10, 11). The question is what happened in studied material between 900°C and 950°C that increased better oxidation resistance of the material. It is known that for pure Fe increase of temperature results in a phase transformation from α -Fe into γ -Fe (at 912°C) [20]. Taking into account the phase transformation and observed differences in the oxidation resistance of studied material, a calculation of diffusion coefficients in the alloy was performed. The diffusion coefficients were approximated based on the literature data from Arrhenius plots. The diffusion coefficients were estimated as follows: for Ni the D_0 ($10^{-4} \text{ m}^2 \text{ s}^{-1}$) = 1.27 and Q (kJ mole^{-1}) = 279.7 [21] and Fe for temperature range 1067-1169K: $D_0 = 121$ and $Q = 281.6$ [22] and for the temperature range 1223-1473K: $D_0 = 4,08$ and $Q=311,1$ [23]. The calculations results revealed that up to 900°C the diffusion coefficient of Fe in the alloy was much higher than for Ni, then at this temperature range formation of Fe-oxide was more likely expected. However, above 900°C, the calculated diffusion coefficient for Fe in the alloy become lower than the calculated diffusion coefficient for Ni. Considering relatively high Ni-content in the studied alloy at the level of 35.5 wt% and higher diffusion coefficient for Ni than for Fe at a temperature above 900°C, then the formation of a more protective oxide scale, namely Ni-rich oxide was expected.

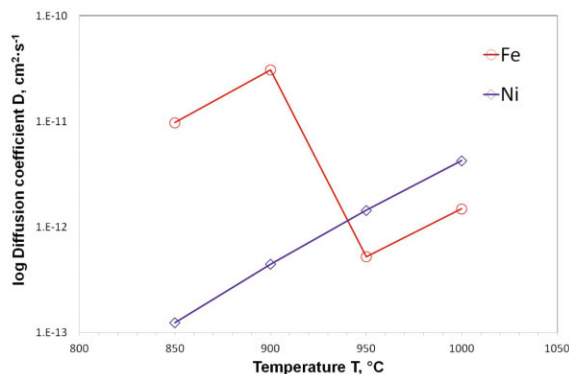


Figure 12. Calculated diffusion coefficients for Ni and Fe at various temperatures

5. Summary and conclusions

In the present work, a ductile iron used as a material for the automotive turbine core was studied at elevated temperatures. Since the efficiency of the turbine depends on temperature, the temperatures used in the present work were far higher than the application temperature. The obtained results allowed to formulate the following conclusions:

- Exposure of the ductile iron at a temperature range 800-900°C resulted in relatively high oxidation

kinetics and an extensive oxide scale spallation;

- Further increase in exposure temperature to 950°C and 1000°C surprisingly resulted in lowering in the oxidation kinetics;

The reason of increased oxidation resistance and better oxide scale adherence was correlated with more prone formation of Ni/Cr/Mn-mixed oxide scale, lower amount of Fe-rich nodules, and formation of Cr/Mn sub-scale; and

- As the reason of the increase in oxidation resistance of ductile iron D5S a phase transformation of Fe at 912°C resulting in change in diffusion coefficients in the alloy for Fe and Ni was concluded, namely the calculated diffusion coefficient in D5S alloy up to 900°C (in α -Fe) the diffusion coefficient for Fe was much higher than for Ni, while at 950°C and 1000°C (in γ -Fe) the opposite situation was found, i.e. diffusion coefficient for Ni was higher than for Fe. The latter is claimed to be the main reason of improvement in oxidation resistance of D5S during air exposure at the temperature above 900°C.

The results obtained in the present work are very promising and can be applied in the real automotive turbine cores as a pre-heat treatment to form a more protective oxide scale and the same suppress the sites for cracks nucleation. However, the latter needs to be investigated as planned in the future.

Acknowledgment

Project financed by the National Center for Research and Development (Narodowe Centrum Badań i Rozwoju) under the TECHMATSTRATEG2/406725/1/NCBR/2020 program.

Data Availability

The datasets generated during and/or analyzed during the current study are available from the corresponding author on reasonable request.

References

- [1] P. P. Milella: Fatigue and corrosion in metals, Springer Verlag, Italia, 2013, p.771-806.
- [2] H. E. Evans, R. C. Lobb, Corros. Sci., 24 (3) (1984) 209-222.
- [3] H. E. Evans, Int. Mater. Rev., 40 (1) (1995) 1-40.
- [4] D. J. Young, High temperature oxidation and corrosion of metals, Elsevier, 2008, p.539.
- [5] K. Matsumoto, M. Tojo, Y. Jinnai, N. Hayashi, S. Ibaraki, Mitsubishi Heavy Industries, Ltd. Technical Review, 45 (3) (2008) 1-5.
- [6] M. Ekström, PhD thesis, KTH Royal Institute of Technology, 2015.
- [7] S. Xiang, B. Zhu, S. Jonsson, Mater. Sci. Forum, 925 (2018) 369-376.



- [8] M.M. Rashidi, M.H. Idris, Mater. Sci. Eng., A, 597 (2014) 395-407.
- [9] R. Covert, J. Morrison, K. Rohrig, W. Spear, Properties and Applications of Ni-resist and Ductile Ni-Resist Alloys, Nickel Development Institute, Reference Book, 1998.
- [10] G. Cao, Z. Li, J. Tang, X. Sun, Z. Liu, High Temp. Mater. Proc., 36(9) (2017) 927-935.
- [11] M. Ekström, S. Jonsson, Mater. Sci. Eng., A, 616 (2014) 78-87.
- [12] M. Ekström, S. Jonsson, Proc. 10th International Symposium on the Science and Processing of Cast Iron – SPCI10, 10-13.11.2014, Mar del Plata, Argentina, p.1-7.
- [13] G.S. Çelik, F. Kahrıman, S.H. Atapek, S. Polat, MATEC Web of Conferences 188 (2018), 02001.
- [14] N. Scheidhauer, C. Dommaschk, G. Wolf, Mater. Sci. Forum, 925 (2018) 393-399.
- [15] M. P. Brady, G. Muralidharan, D. N. Leonard, J. A. Haynes, R. G. Weldon, R. D. England, Oxid. Met., 82 (2014) 359-381.
- [16] M. Ekstrom, P. Szakalos, S. Jonsson, Oxid. Met., 80 (2013) 455-467.
- [17] M. Schütze, W.J. Quadackers, Oxid. Met., 87 (2017) 681-704.
- [18] P. Y. Hou, R. M. Cannon, Oxid. Met., 71 (2009) 237-256.
- [19] J. A. Haynes, B. A. Pint, W. D. Porter, I. G. Wright, Mater. High Temp., 21(2) (2014) 87-94.
- [20] J. Meiser, H.M. Urbassek, Metals, 8 (2018) 837.
- [21] R.E. Hoffman, F.W. Pikus, R.A. Ward, Trans AIME, 206 (1956) 483.
- [22] J. Fillon, D. Calais, J. Phys. Chem. Sol., 38 (1977) 81.
- [23] I.G. Ivantsov, A.M. Blinkin, Fiz. Met. Metalloved, 22 (1966) 876.

POVEĆANJE IZDRŽLJIVOSTI AUSTENITNOG DUKTILNOG GVOŽĐA TIP A D5S POSTUPKOM PRETHODNE OBRADNE NA VISOKOJ TEMPERATUR I

W. J. Nowak ^{a*}, B. Wierzb a, A. Mazurkow ^a, A. Jaworski ^b, L. Krawczyk ^b

^{a*}Odsek za nauku o materijalima, Fakultet za mašinsko inženjerstvo i vazduhoplovstvo, Tehnološki univerzitet u Žešovu, Žešov, Poljska

^bBorgWarner Turbo Systems, BorgWarner Poljska, Tehnički centar u Žešovu, Poljska

Apstrakt

U ovom radu je ispitivano ponašanje ASTM A439 austenitnog duktilnog gvožđa tipa D5S na visokim temperaturama u oksidacionom okruženju. Dobijeni rezultati su pokazali da je izlaganje temperaturama od 800°C, 850°C i 900°C dovelo do relativno visokog porasta mase i opsežne spalacije oksidnog sloja na površini uzoraka tokom hlađenja. Međutim, izloženost materijala na temperaturi od 950°C je dovela do bolje otpornosti na oksidaciju, a spalacija oksidnog sloja se nije dogodila. Materijal izložen temperaturi od 1000°C je pokazao najbolju otpornost na oksidaciju među ispitivanim uzorcima. Ispitivanje površine i poprečnog preseka je pokazalo da se na materijalu izloženom temperaturi od 950°C uglavnom formirao Ni/Cr/Mn zaštitni oksidni sloj i grumeni bogati gvožđem. U poređenju sa uzorkom koji je izložen temperaturi od 1000°C, manja količina grumena bogatog gvožđem je primećena po jedinici površine i veći deo površine je bio prekriven Ni/Cr/Mn zaštitnim slojem. Ovo poslednje se objašnjava promenom izračunatih koeficijenata difuzije za Ni i Fe u leguri, gde je do 900°C koeficijent difuzije za Fe bio mnogo viši nego za Ni, dok je iznad 900°C koeficijent difuzije za Ni bio veći nego koeficijent difuzije za Fe. Ova pojava je povezana sa faznom transformacijom Fe iz α -Fe u γ -Fe, što je kao rezultat imalo promenu koeficijenta difuzije.

Ključne reči: Duktilno gvožđe; Kinetika oksidacije; Kućište automobilske turbine; Dugotrajna modifikacija; Uticaj temperature

